PAMUKKALE ÜNİVERSİTESİ
Mühendislik Bilimleri Dergisi

PAMUKKALE UNIVERSITY
Journal of Engineering Sciences

Araştırma makalesi | Research paper

Cilt | Vol: XX • Sayı | No: X • ss | pp: XXXX-XXXX • Yıl | Year: 20XX

MIMO microstrip antenna design and production for 5G applications

Miraç Er [1], Nursel Akçam [2]

ARTICLE INFO

Dates:
Received: 02.03.2026
Accepted: 22.06.2026

Doi:
10.65206/pajes.1901295

Corresponding author:
Nursel Akçam
(ynursel@gazi.edu.tr)

Author addresses:
[1] ASELSAN A.Ş., Ankara, 06570, Türkiye
(mirac.er23@gmail.com)

[2] Department of Electrical & Electronic Engineering, Faculty of Engineering, Gazi University, Ankara, 06570, Türkiye.
(ynursel@gazi.edu.tr)

ABSTRACT

Context—In recent years, the increasing need for communication due to technological advancements, along with the rise in the number of manufacturers and users, has made the transition to 5th generation (5G) communication systems necessary. This transition to 5G communication has placed new requirements on antenna designs, necessitating the development of antennas with high bandwidth, a low profile, and the ability to support multiple users simultaneously. This paper focused on increasing the bandwidth of multiple input multiple output (MIMO) microstrip antennas and improving the isolation between ports.

Objective—This article describes the design and fabrication of a low-profile, high-bandwidth, dual-polarization, four-port, 1×2 array microstrip MIMO antenna for systems operating at 5G frequencies. The designed antenna is manufactured, and its measurement results are compared with simulation results. To enable the proposed design to operate in dual polarization, two ports were placed perpendicular to the edges of the patch antenna. The patches are designed in a square shape to ensure the antenna has linear polarization and exhibits equal characteristics in both horizontal and vertical polarizations. It is aimed at the MIMO antenna to operate at a minimum of 25 GHz - 26 GHz range, linearly in dual polarization, and to have better than -20 dB isolation between ports despite the placement of patch structures with a distance 0.25λ. To increase the antenna bandwidth and improve isolation between ports, the defected ground structure (DGS) method and neutralization line method are employed in the design. The antenna is 2.4 cm × 2.96 cm in size and has 4 ports, achieves a bandwidth of 2.33 GHz with 7 dBi gain at two ports for horizontal polarization, and a bandwidth of 3.5 GHz with 9.18 dBi gain at two ports for vertical polarization. Additionally, the targeted isolation values between ports in the 25 GHz - 26 GHz range are achieved to be better than -20 dB. The designed MIMO antenna is also evaluated in terms of important MIMO parameters such as diversity gain (DG), envelope correlation coefficient (ECC), total active reflection coefficient (TARC), and channel capacity loss (CCL).

Method—In the designed antenna, an RT/duroid 5880 substrate with a dielectric constant (ε_r) of 2.2, a loss tangent (tan δ) of 0.0009, and a thickness of 0.787 mm has been used. A 1 oz (0.035 mm) thick layer of copper was used on both the bottom (grounding plane) and top (radiation area) surfaces of the dielectric material.

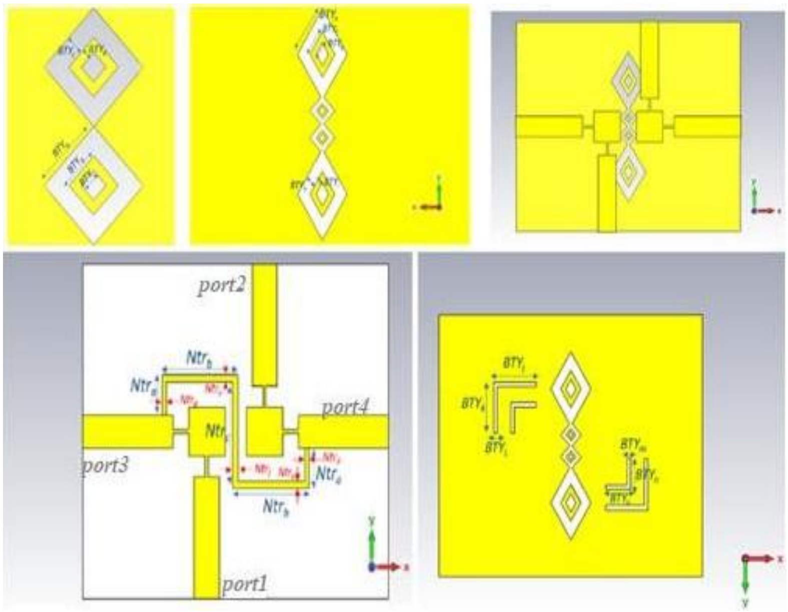

Results—To minimize the antenna's footprint, the patch structures were placed at a distance 0.25λ apart, while ensuring that the isolation between the ports remains below -20 dB. The bandwidths of the 4-port antenna were measured as 3.89 GHz, 4.72 GHz, 4.35 GHz, and 3.8 GHz respectively. Consistency was observed between the data obtained from measurements and simulation results.

Conclusion—CST Microwave Studio simulation software was used for design and simulations.

Key Words— Defected ground structure, Microstrip antenna, MIMO, Neutralization line.

I. INTRODUCTION

In the ever-evolving landscape of technology, the rising need for communication, alongside the expanding base of producers and users, has become necessary advancements in communication. Modern mobile wireless communication standards are being developed to meet this demand for more advanced communication solutions [1]. The ongoing usage of the 4G standard has led to a scenario where it is increasingly unable to meet users' expectations for low latency, high data rate and high bandwidth, as well as supporting multiple user and fast data transfer. It is observed that spectral efficiency of the frequency band allocated for 4G communication has decreased is evident due to the increasing demands in communication [2]. The unmet expectations of users have been instrumental in the emergence of the 5G standard. The standardization process of 5G communication is still ongoing, with expectations that it will support high data rate, have high channel capacity, provide low latency and low power consumption in data transmission. Additionally, it is anticipated that 5G will utilize frequency spectrums between 24 GHz and 71 GHz, often referred to as millimeter wave bands [2], [3]. The implementation of 5G communication has necessitated the development of antenna technologies as well as the developments in communication technologies. To meet the requirements expected from 5G technology, antenna solutions that can operate at relevant frequencies, support high bandwidths, have high gain and support multiple users at the same time are needed. The fulfillment of all these requirements has necessitated the use of MIMO antennas alongside 5G communication [3].

In the literature, it is seen that MIMO antennas generally offer a low profile, easily produced and cost-effective solution, and microstrip antennas are preferred in array structures. Microstrip antenna, also known as a patch antenna, radiates with a conductive surface called a patch on its top surface, which has one or more dielectric substrate layers between the conductive materials on its top and bottom surfaces. Although this type of antenna, designed in various geometric shapes, offers many feeding methods and is often preferred, it tends to have relatively low bandwidth and gain [4], [5]. Due to these disadvantages, antenna designs often aim to minimize them by using thick substrate materials, low dielectric constant substrates, or multi-layer structures with multiple substrate surfaces. In addition to these methods, in recent years, antenna designs have also utilized the defected ground structure (DGS) method to increase bandwidth and achieve port isolation in MIMO antennas. Moreover, there are antenna designs obtained by using a neutralization line to combine two ports through a single line to enhance performance [6], [7]. Especially in high frequency applications, DGS technique is used to reduce mutual coupling, suppress cross polarization, increase frequency bandwidth and increase gain [3], [8]-[10]. Although the slots opened on the ground surface have simple or complex geometries, they are frequently used in literature [8], [11]. Neutralization lines are designed depending on factors such as distance between antennas, placement and location of antennas. A properly designed neutralization line increases performance in MIMO systems and minimizes unwanted interactions [6], [7]. According to [11], there are two main characteristics of DGS; these are the operating and stop band characteristics of the antenna. When the literature is examined, it is observed that some studies are designed for the lower band of 5G frequencies and generally have low bandwidth, and those that do not have an array antenna structure have low gain values [10], [12], [13]. It is observed that some antennas designed for the upper band of 5G frequencies have low bandwidth and gain values are low because they are not in an array structure [9], [14]-[16]. However, in studies where the DGS method or neutralization line is added, it is observed that the bandwidth increases and the isolation values between ports improve [6], [7], [17]. In this article, a manufacturable antenna which is 2.4 cm × 2.96 cm dimensions, using Rogers RT5880 (0.787 mm) dielectric material, operating in mm-wavelength broadband, 2-element, 4-port, dual (horizontal and vertical) polarized, with DGS and neutralization line design and production has been carried out. Measurements of S-parameters were made through a network analyzer and bandwidth, and port isolation values were compared with simulation results.

II. ANTENNA DESIGN and SIMULATION RESULTS

In the designed antenna, an RT/duroid 5880 substrate with a dielectric constant (ε_r) of 2.2, a loss tangent ($\tan\delta$) of 0.0009, and a thickness of 0.787 mm has been used [9]. Copper material with a thickness of 1 oz (0.035 mm) is used on the bottom surface of the dielectric material, which serves as the ground plane, and on the top surface of the dielectric material, which is used as the radiation area. CST Microwave Studio simulation software was used for the design and simulations.

A. Single-element antenna design

Within the scope of this article, to achieve the proposed MIMO antenna design, first the parameters of the single-element antenna were determined, and its simulations were performed. For the single-element antenna design, the dimensions of the patch antenna, the dimensions of the feed line, and the dimensions of the quarter-wave transformer to achieve a 50 Ω impedance were determined. The parameters to be used in the single-element antenna design were determined by (1)-(10) [18] and the values are given in Table 1. To enable the antenna to operate in dual polarization, two ports were positioned orthogonally to each other, with the ports placed exactly at the center of the patch edges to prevent polarization distortion. Additionally, to ensure that the antenna has linear polarization and possesses equal characteristics in both linear polarizations (horizontal and vertical polarization), it was decided that the patch should have a square geometry.

Width of patch antenna is defined by

$$W_p = \sqrt{2/(\varepsilon_r+1)}\big/\left(2f_r\sqrt{\varepsilon_0\mu_0}\right) = v_0\sqrt{2/(\varepsilon_r+1)}\big/(2f_r) \qquad (1)$$

Reference epsilon value is defined by

$$\varepsilon_{reff} = [(\varepsilon_r+1)/2] + [(\varepsilon_r-1)/2]\left[1+12\left(h/W_p\right)\right]^{-1/2}. \qquad (2)$$

Delta length due to fringing is defined by

$$\frac{\Delta L}{h} = 0.412\frac{(\varepsilon_{reff}+0.3)\left[(W_p/h)+0.264\right]}{(\varepsilon_{reff}-0.258)\left[(W_p/h)+0.8\right]}. \qquad (3)$$

Length of patch antenna is defined by

$$L_p = \left[1/\left(2f_r\sqrt{\varepsilon_{reff}}\sqrt{\varepsilon_0\mu_0}\right)\right] - 2\Delta L. \qquad (4)$$

Characteristic impedance of the antenna is defined by

$$Z_a = [90\varepsilon_r^2/(\varepsilon_r-1)]\left(L_p/W_p\right)^2. \qquad (5)$$

Characteristic impedance of quarter wavelength transmission line is defined by

$$Z_q = \sqrt{Z_0 Z_a}. \qquad (6)$$

Table 1. Single element small size antenna parameters.

Parameter	Explanation	Value (mm)
W_p	Width of patch antenna	3.5
L_p	Length of patch antenna	3.5
W_s	Width of dielectric structure	9
L_s	Length of dielectric structure	9
W_q	Width of quarter wavelength transmission line	0.275
L_q	Length of quarter wavelength transmission line	1.5
W_{50}	Width of 50 Ω transmission line	2.4
L_{50}	Length of 50 Ω transmission line	1.25
h	Thickness of dielectric structure	0.787
t	Thickness of copper surfaces	0.035

Width of quarter wavelength transmission line is defined by

$$Z_q = (60/\sqrt{\varepsilon_r})\ln[(8h/W_q) + (W_q/4h)]. \tag{7}$$

Length of quarter wavelength transmission line is defined by

$$L_q = \lambda/4. \tag{8}$$

Width of 50 Ω supply line is defined by

$$Z_0 = 120\pi/\sqrt{\left\{\varepsilon_{reff}\left[1.393 + \frac{W_{50}}{h} + \frac{2}{3}\ln\left(\frac{W_{50}}{h} + 1.444\right)\right]\right\}}. \tag{9}$$

Length of 50 Ω supply line is defined by

$$L_{50} = (L_p/\pi)[\cos^{-1}(\sqrt{Z_0/Z_q})]. \tag{10}$$

In equations (1)-(10), μ_0 is the free space permeability; ε_0 is the free space permittivity; ε_r is relative permittivity; f_r is operating frequency; v_0 is free space velocity; Z_0 is supply line characteristic impedance and λ is wavelength.

Since the designed antenna was aimed to be manufacturable, the connector to be used was determined as the SF1621-60036 connector of the SV Microwave in accordance with the antenna operating frequency, and the length of the 50 Ω transmission line of the antenna and the antenna dimensions were recalculated. As a result of the calculation, the manufacturable single-element antenna given in Fig. 1 was designed by taking $W_s = L_s = 24$ mm, $L_{50} = 8.75$ mm, different from the values given in Table 1, and its S-parameters were obtained (Fig. 2). $S11$ values refer to the reflection coefficient of the antenna. For a proper communication, it is desired that the $S11$ parameters should be well below −10 dB.

B. Two-element antenna design

A second antenna with similar dimensions to the single-element two-port antenna was placed at a distance 0.25λ from the first antenna, and the dielectric and ground surface dimensions were readjusted to obtain the MIMO antenna design shown in Fig. 3.

Simulations were made for the resulting 4-port, MIMO, dual polarization antenna and the S-parameter results given in Fig. 4 and Table 2 were obtained. When the results in Table 2, given as reference to the 25.5 GHz value, which is the midpoint of the 25 - 26 GHz range in the isolation values between ports, are examined,

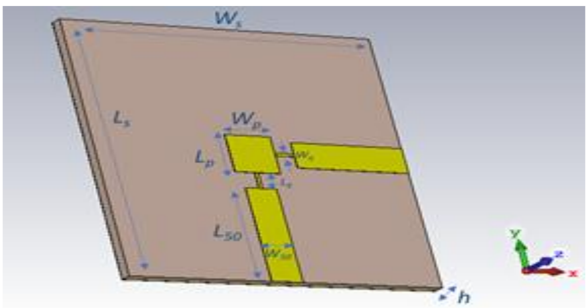

Fig. 1. Manufacturable single-element antenna.

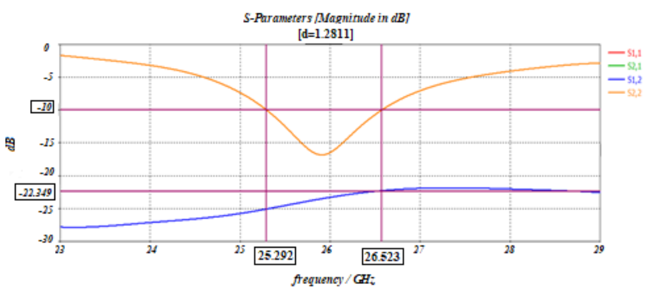

Fig. 2. S-parameter graph of manufacturable single-element antenna.

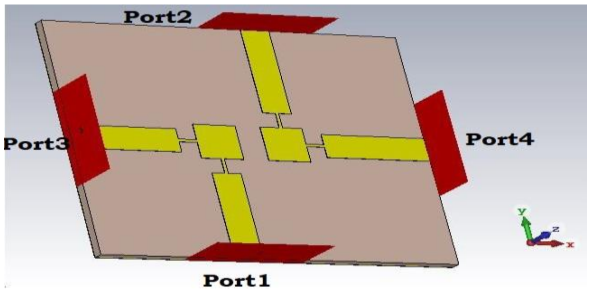

Fig. 3. First designed MIMO antenna with port number.

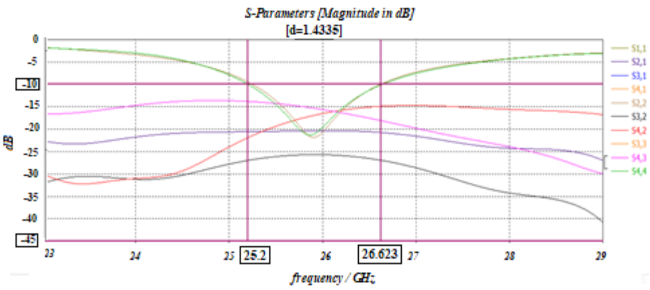

Fig. 4. S-parameter results of the first designed MIMO antenna.

it is observed that the isolation between some ports is greater than -20 dB. When the gain values of the antenna given in Fig. 5 and Table 2 are examined, it is observed that the antenna gain is better than 8 dBi and the beams are not scattered, and the antenna gain is concentrated in a certain region. However, it was observed that the bandwidths of the ports were low.

C. Improvement of designed MIMO antenna parameters

In the ongoing design process, studies were carried out on adding the DGS method and neutralization line to the antenna to improve the isolation between ports and increase the bandwidth.

Table 2. Simulation results of the first designed MIMO antenna.

S-parameter	Value (dB)	Bandwidth (GHz)	Gain (dBi)
S11	<-10	1.38	8.18
S22	<-10	1.38	8.18
S33	<-10	1.44	8.33
S44	<-10	1.44	8.33
S21	-20.48		
S31	-19.35		
S41	-26.12		
S32	-26.12		
S42	-19.35		
S43	-14.28		

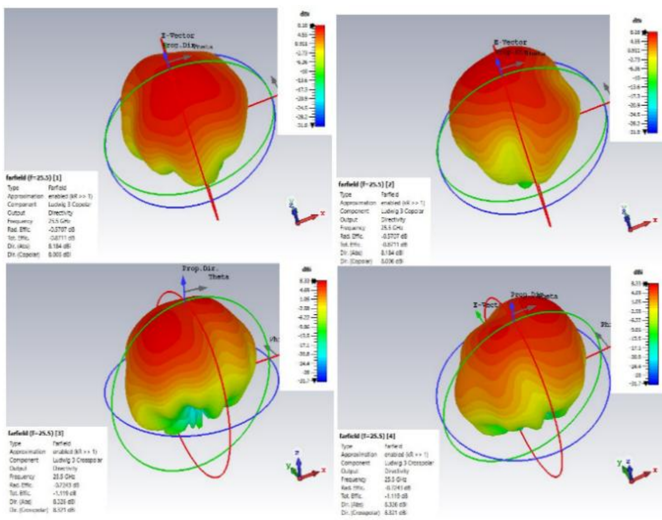

Fig. 5. Gain simulation results of the ports of the first designed MIMO antenna.

When applying the DGS method to the ground surface of the antenna, many complex geometric shapes tested in the literature were tried on several strategically important points affecting the antenna parameters; for example, the backs of the patches, the backs of the feed lines, the junction points of the feed lines and patches, etc. However, the expected effect on the antenna parameters from the geometric patterns carved into the ground surface of the antenna was not observed. Subsequently, it was observed that modifications made in the region on the ground plane projection of the region between two patches, a strategic point, positively impacted the antenna parameters (Fig. 6a). In this case, choices were made among geometric structures, and it was evaluated that the most suitable shape was the shape formed by rotating the square structure 90 degrees clockwise, and the dimensions should be *BTYa* = 1.6 mm, *BTYb* = 0.8 mm, *BTYc* = 0.4 mm, *BTYd* = 0.2 mm (Fig. 6b). The same geometric shape continued along the y-axis and parametric analyzes were continued. Considering the length-width balance of the feed line with 50 Ω impedance, the square geometry was slightly changed, and the structure was obtained which is shown in Fig. 6c. The values in the newly added structure are designed to be *BTYe* = 4.08 mm, *BTYf* = 2.04 mm, *BTYg* = 1.02 mm, *BTYh* = 0.98 mm, *BTYı* = 0.51 mm.

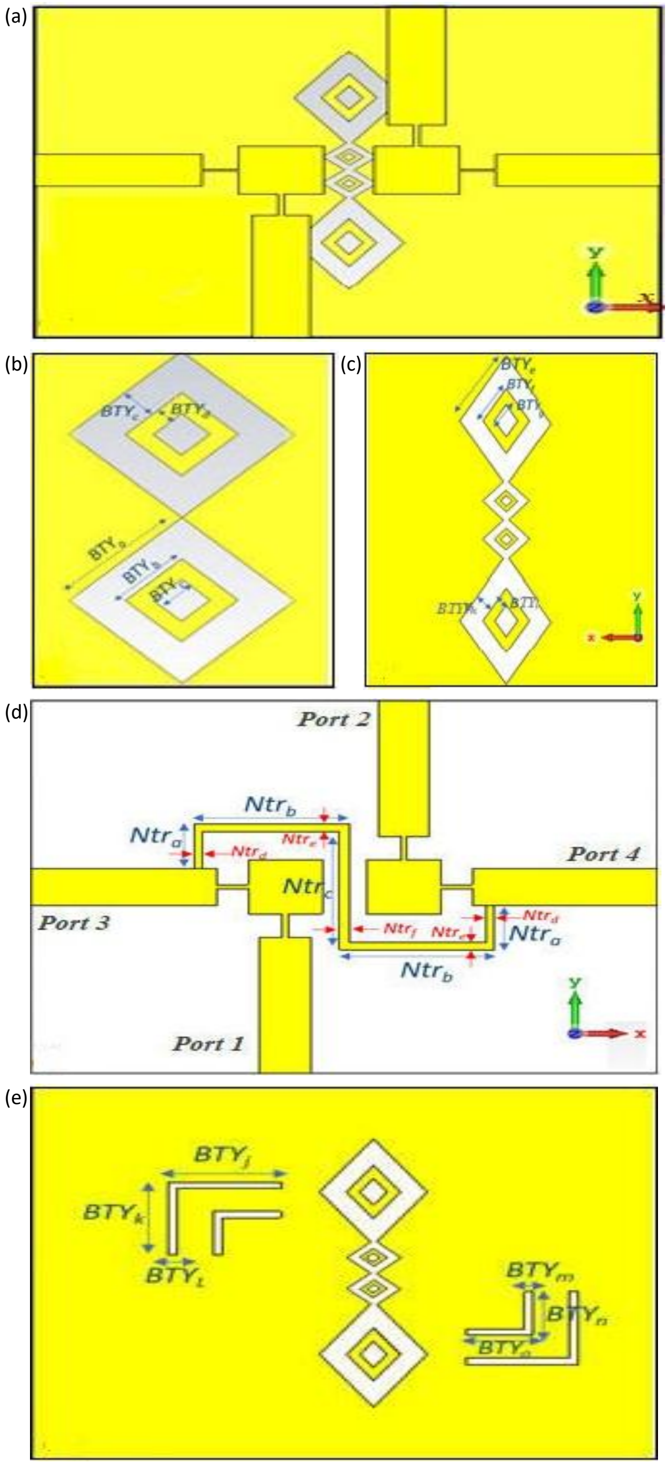

Fig. 6. (a), (b), (c) Added all DGS geometries, (d) Neutralization line, (e) Final design.

When examining the values in Table 3 (with DGS method), which was created by referencing the 25.5 GHz value (the midpoint of the 25-26 GHz range) to determine the between ports isolation in the S-parameter graph of the DGS-containing antenna given in Fig. 7a, it was observed that the geometric patterns opened on the ground surface increased the bandwidth of ports 1 and 2, reduced the S11 and S22 values to below -50 dB, and although it did not change the bandwidth of ports 3 and 4, it reduced the S33 and S44 values to below -35 dB. However, it was observed that the geometric patterns added to the ground surface had no effect on the port isolations.

In the continuation of the design, a neutralization line was added to increase the bandwidth of the 3rd and 4th ports and to improve the isolation between the ports. The parameters of the added neutralization line are designed to be *Ntra* = 2.85 mm,

Table 3. S-parameter values of designed antenna.

Design method	S-Parameter	Value (dB)	Bandwidth (GHz)
DGS	S11	<-10	2.14
	S22	<-10	2.14
	S33	<-10	1.38
	S44	<-10	1.38
	S21	-20.06	
	S31	-18.38	
	S41	-23.61	
	S32	-23.61	
	S42	-18.38	
	S43	-17	
DGS and neutralization line	S11	<-10	1.94
	S22	<-10	1.94
	S33	<-10	1.92
	S44	<-10	1.92
	S21	-20.6	
	S31	-19.28	
	S41	-24.32	
	S32	-24.32	
	S42	-19.28	
	S43	-20.36	

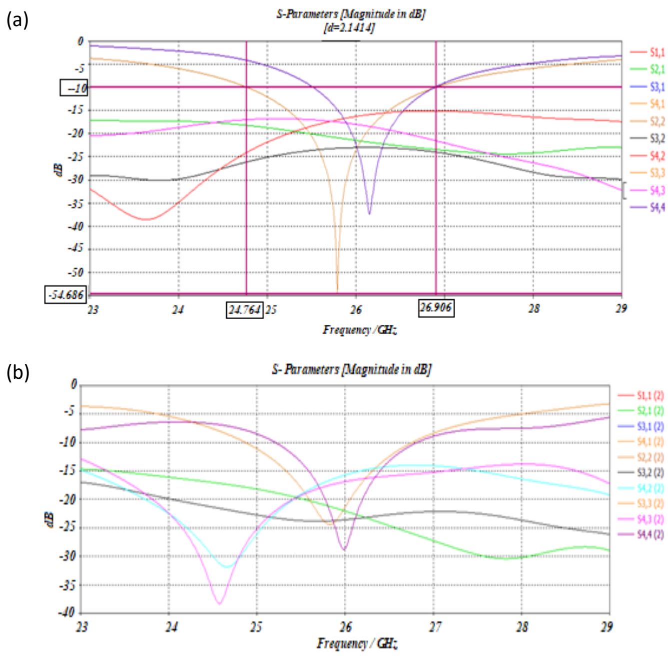

Fig. 7. S-parameters of designed antenna: (a) with DGS, (b) with DGS and neutralization line.

Ntrb = 7.32 mm, *Ntrc* = 7.63 mm, *Ntrd* = 0.375 mm, *Ntre* = 0.475 mm, *Ntrf* = 0.475 mm. In the final stage of the design, a new DGS structure was added to reduce the isolation values of ports with higher than -20 dB values in the 25 - 26 GHz range to below -20 dB (Fig. 6d). The dimensions of this structure, which resembles an "L" shape, are determined as *BTYj* = 4.75 mm, *BTYk* = 4.64 mm, *BTYL* = 0.375 mm, *BTYm* = 0.375 mm, *BTYn* = 2.74 mm, *BTYo* = 2.85 mm. All added DGS geometries and neutralization line are given in Fig. 6e, and the design phase is finalized.

The S-parameter graph for the design given in Fig. 6d is shown in Fig. 7b. Although the between ports isolation values in the 25-26 GHz range appear to remain largely unchanged in Table 3 (with DGS and neutralization line methods), Fig. 7b shows that the bandwidth of ports 3 and 4 increases with the addition of the neutralization line, and the between port isolation curves trend downwards. Specifically, it is observed that the S42 and S43 curves reach their minimum values between the 24-25 GHz frequencies. The physical placement of the DGS slots along the y-axis creates an anisotropic boundary condition on the shared ground plane (Fig. 6a). Physically, when individual ports are active, the surface currents tend to couple through the shared ground plane primarily along the y-axis. The integration of the DGS oriented in the y-direction serves as a slotline-like band-stop resonator. This orientation blocks the y-polarized electric fields and cuts off the direct path of the surface currents between the adjacent port pairs. Consequently, the mutual coupling is heavily suppressed, forcing the surface currents to redistribute away from the neighboring feeds.

In the final stage of the design, it was decided to add a new DGS structure to reduce the isolation values to below -20 dB. Before adding the DGS structure, it was observed that the area between the adjacent ports of the antenna was suitable and that structures resembling an "L" shape had a significant effect on the antenna parameters because of parametric analyses (Fig. 6e). As a result of the analyses, the optimum dimensions were determined as *BTYj* = 4.75 mm, *BTYk* = 4.64 mm, *BTYL* = 0.375 mm, *BTYm* =0.375 mm, *BTYn* = 2.74 mm, *BTYo* = 2.85 mm.

Simulations were made with the final designed antenna, and the S-parameter results given in Table 4 and Fig. 8 were obtained. When the results are examined, it is observed that the bandwidths have increased significantly and the isolations between ports have reached the lowest values in the 25 - 26 GHz range. When the comparison table given in Table 4 is examined, it is observed that there is a significant improvement in terms of bandwidth and port isolation between the antenna in which the DGS method and neutralization line are not added and the final designed antenna.

Table 4. S-parameter results comparison table of the final designed antenna and with the first designed MIMO antenna.

PM	First Designed	Final Designed	Inc. Rate (%)
S11	<-10 dB, 1.38 GHz (BW)	<-10 dB, 2.33 GHz (BW)	68.84
S21	-20.3 dB	-24.5 dB	19.63
S31	-14.9 dB	-27.03 dB	39.7
S41	-25.7 dB	-28.3 dB	8.34
S22	<-10 dB, 1.38 GHz (BW)	<-10 dB, 2.33 GHz (BW)	68.84
S32	-25.7 dB	-28.3 dB	8.34
S42	-14.9 dB	-27.03 dB	39.7
S33	<-10 dB, 1.44 GHz (BW)	<-10 dB, 3.5 GHz (BW)	143.05
S43	-13.8 dB	-34.26 dB	139.91
S44	<-10 dB, 1.44 GHz (BW)	<-10 dB, 3.5 GHz (BW)	143.05

PM: Parameter, BW: Bandwidth, Inc. Rate: Increasing rate

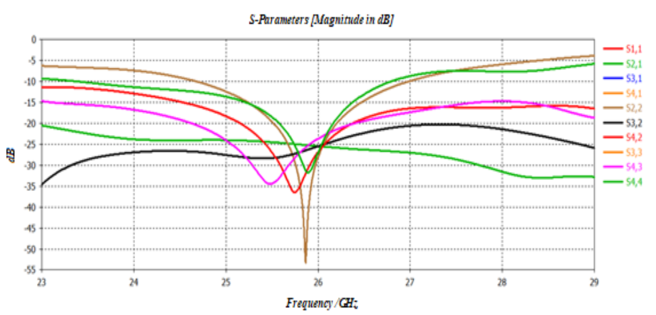

Fig. 8. S-parameter results of the final designed antenna.

When the values given in Table 5 and Fig. 9 are examined, it is observed that the gain values for port 1 and port 2 decreased by 1.18 dBi because of the added DGS and neutralization line. On the other hand, the gain values for port 3 and port 4 increased by 0.85 dBi. Also, when the beams in Fig. 9 are analyzed, it is seen that they are more scattered compared to the beams given in Fig. 5.

D. Produced antenna and measurement results

Within the scope of this study, the goal is to design a producible, 4-port, dual-polarized antenna improved with DGS and neutralization line techniques. In this context, the antenna, whose design was completed in the previous section, simulation results obtained, and final form given in Fig. 10, has been produced.

S-parameter measurements of the manufactured antenna were compared with simulation results, as shown in Fig. 11. Tables 6 and 7 show that the measurement results and simulation results are close to each other. A slight frequency shift and discrepancy in magnitude are observed between the simulated and measured S-parameters. Physically, this behavior is a well-known phenomenon in antenna fabrication, stemming from the manufacturing tolerances of the substrate's dielectric constant, copper thickness, and manual soldering variations of the SMA connectors. To evaluate its impact on performance, operating efficiency was investigated. Although the actual dielectric losses slightly reduced the measured peak radiation efficiency compared to the simulation, the total efficiency remains highly acceptable within the targeted band, since the measured reflection coefficient safely satisfies the Sii < 10 dB criteria. When the results of S11, S22, S33 and S44 are examined, it is observed that the resonance frequency of the antenna has shifted slightly, due to millimetric errors occurring in production and the frequency-dependent changing characteristics of the connector used creating a big difference during simulation and

Table 5. Gain simulation results comparison table of the final designed antenna and with the first designed MIMO antenna.

Port Number	Gain (dBi)	
	First Designed Antenna	Final Designed Antenna
Port 1	8.18	7
Port 2	8.18	7
Port 3	8.33	9.18
Port 4	8.33	9.18

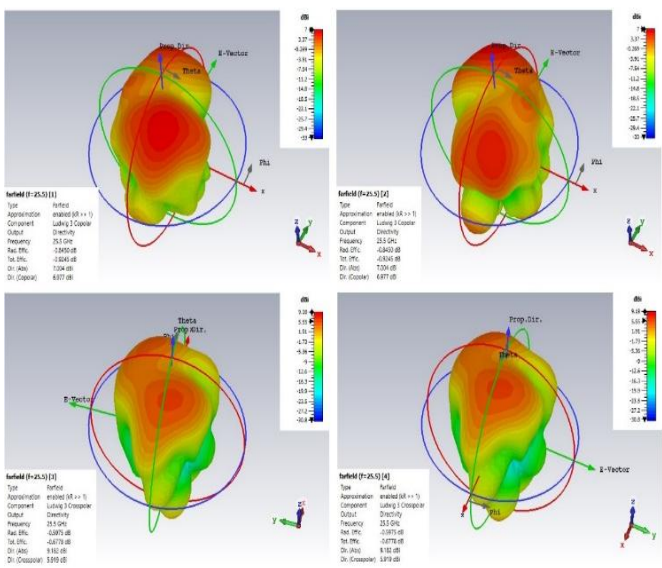

Fig. 9. Gain simulation results of the ports of the final designed antenna.

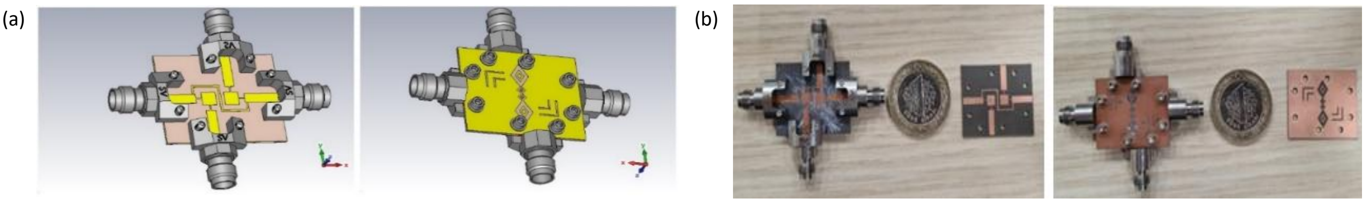

Fig. 10. Designed and producted antenna: (a) Connector version, (b) Producted version.

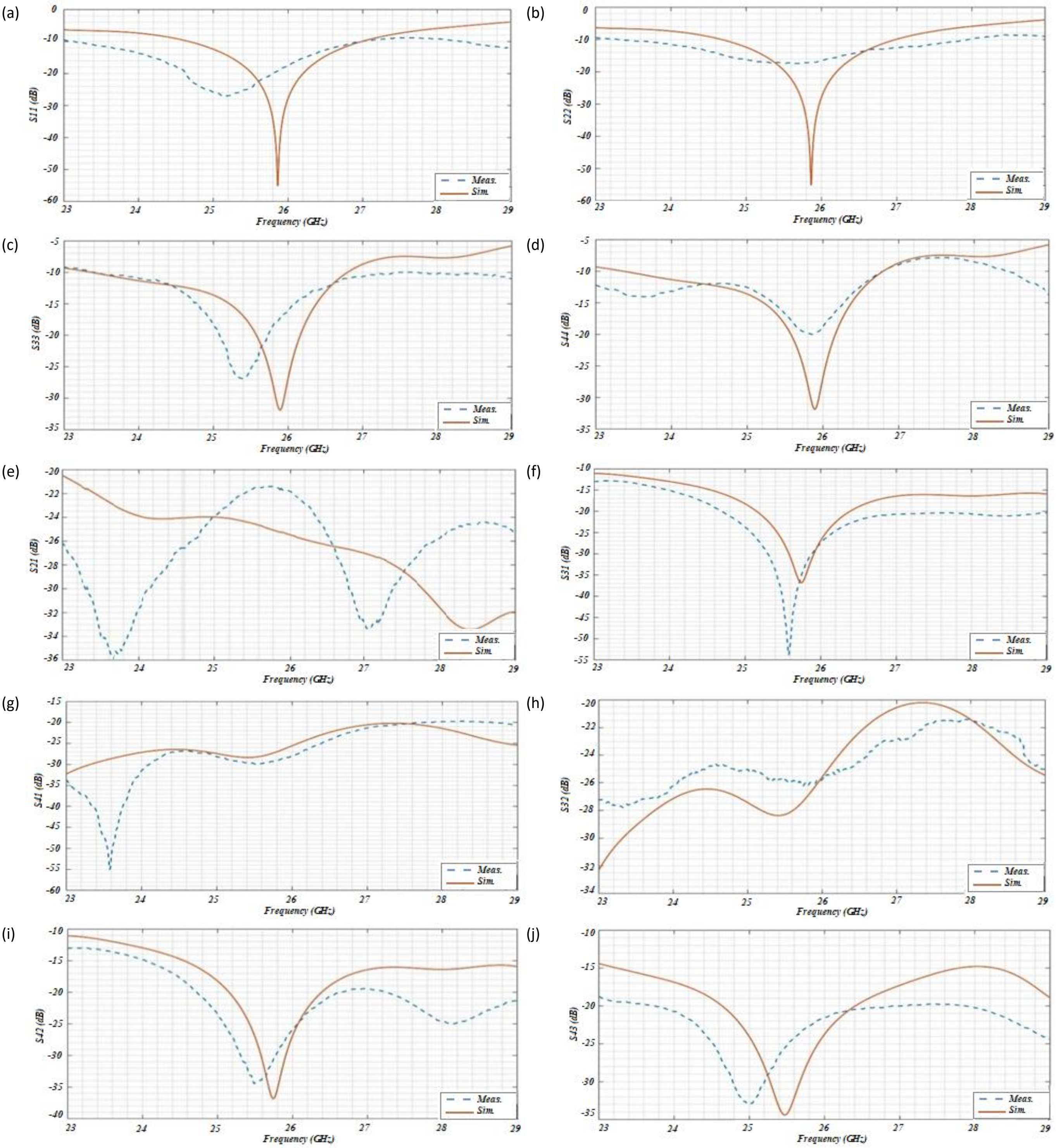

Fig. 11. Measurement and simulation results of S-parameters: (a) S11, (b) S22, (c) S33, (d) S44, (e) S21, (f) S31, (g) S41, (h) S32, (i) S42, (j) S43.

measurement. However, it is observed that the bandwidths of the ports are high as targeted. As can be seen from the graphics, the bandwidths resulting from the measurement of the third and fourth ports cannot be determined exactly. For this reason, minimum values are given in Table 6. When the S-parameters expressing the isolation values between ports given in Figs. 11e-11j and Table 7 are examined, it is observed that the measurement results are largely converged to the simulation results, and in addition, the isolation values between ports remain below -20 dB as targeted.

Table 6. Center frequency values for S11, S22, S33 and S44 and bandwidth of the region below -10 dB.

Port Number	Central Frequency, GHz (Simulation)	Center Frequency, GHz (Measurement)	BW, GHz (Simulation)	BW, GHz (Measurement
Port 1	25.87	25.12	2.33	3.89
Port 2	25.86	25.33	2.33	4.72
Port 3	25.38	25.89	3.50	>4.35
Port 4	25.87	25.90	3.50	>3.80

Table 7. Isolation values between ports.

S-Parameter	Sim. Results, dB (25.5 GHz)	Meas. Results, dB (25.5 GHz)
S21	-24.50	-22.50
S31	-27.03	-43.98
S41	-28.30	-29.71
S23	-28.30	-25.77
S42	-27.03	-34.50
S43	-34.26	-25.27

The isolation performance between different port pairs exhibits a variation from 22.5 dB to 43.98 dB. This behavior can be modeled by the combined effects of spatial positioning and polarization orthogonality. For example, S21 exhibits the minimum isolation of 22.5 dB due to the strong mutual coupling of surface currents over the compact shared substrate. On the other hand, the orthogonal placement ports (e.g. S31) suppress the field interaction, yielding an excellent isolation of 43.98 dB. It is important to emphasize that even the minimum isolation value (22 dB) complies safely with the requirements of modern wireless standards.

There are some other important parameters such as envelope correlation coefficient (ECC), diversity gain (DG), total active reflection coefficient ($TARC$), and channel capacity loss (CCL) that provide information about MIMO antenna performances [19]-[24].

ECC is one of the basic parameters of MIMO systems. It specifies how the antenna elements are mutually coupled to each other and its analysis is performed by using (11) reported in [25]:

$$ECC = \frac{\left|\iint_{4\pi} \vec{E_1}(\theta,\emptyset).\vec{E_2}(\theta,\emptyset)\, d\Omega\right|^2}{\left(\iint_{4\pi}\left|\vec{E_1}(\theta,\emptyset)\right|^2 d\Omega\right)\left(\iint_{4\pi}\left|\vec{E}_2(\theta,\emptyset)\right|^2 d\Omega\right)}, \quad (11)$$

where $\vec{E}_i(\theta,\emptyset)$ refers to the electric field radiated by the ith antenna element with the other antenna element terminated by a 50 Ω load, and $d\Omega = sin\theta d\theta d\emptyset$ is solid angle.

DG shows the loss of transmit power without loss of performance when diversity schemes are presented for MIMO configuration. DG is calculated from the ECC value using (12):

$$DG = 10\sqrt{1-|ECC|}, \quad (12)$$

The TARC-based radiation efficiency can consider the effect when ports of the multiple antennas system are fed with signals of different phases simultaneously. The TARC general formulation for N port transmission is defined in (13):

$$TARC = \sqrt{\textstyle\sum_{n=1}^{N}|P_{rn}|^2}\Big/\sqrt{\textstyle\sum_{n=1}^{N}|P_{in}|^2}, \quad (13)$$

where P_{rn} is reflected power and P_{in} is incident power [26]. The TARC is defined by (14) for 4-port antenna in terms of S-parameters, as follows [26]:

$$TARC = \frac{1}{2}\sqrt{\textstyle\sum_{k=1}^{4}\left|Sk1 + \sum_{l=2}^{4} Skle^{j\theta l}\right|^2}. \quad (14)$$

The CCL sets the maximum achievable message transmission rate limit of the signal that can be continuously transmitted over the communication channel with a loss less than 0.4 bit/s/Hz in the operating frequency range during the correlation effect. The CCL curve of the proposed antenna is derived from (15) and (16) [3]:

$$C_{loss} = -\log_2 \det(\mathbf{A}), \quad (15)$$

where the matrix $\mathbf{A} = \left[a_{ij}\right]_{1\le(i,j)\le 4}$ is defined by

$$a_{ij} = \begin{cases} 1-\sum_{n=1}^{N}|Sin|^2, & i=j \\ -Sii^{*}Sij + Sjj^{*}Sij, & i\neq j \end{cases}. \quad (16)$$

The ECC, DG, $TARC$ and CCL curves of the proposed MIMO antenna are given by Fig. 12. It appears from Fig. 12b that the DG approaches the ideal value of 10 dB. From Figs. 12a and 12b, the DG and ECC curves are in consonance, i.e., the DG curve approaches 10 dB when the ECC curve moves toward zero, and vice versa [27]. It is observed that TARC curve is also found to be within the acceptable limit (< −10 dB in the operating bands) for

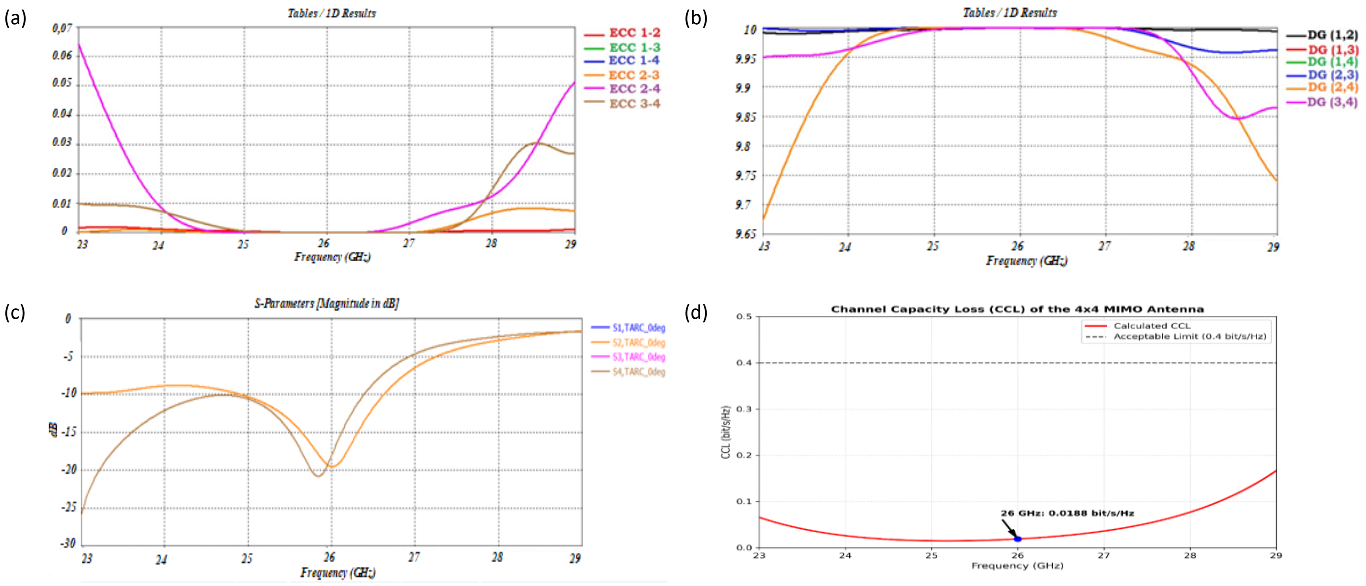

Fig. 12. Performance parameters of the proposed MIMO antenna: (a) ECC values, (b) DG values, (c) $TARC$ values, (d) CCL values.

the proposed MIMO antenna. Overall, the proposed antenna presents a good degree of MIMO characteristics and establishes an excellent trade-off between all performance parameters ECC, DG, $TARC$, and CCL of the antenna.

E. Discussion

To closely investigate the physical mechanism behind broadband performance, a detailed parametric study was conducted. This parametric study demonstrates the increase in bandwidth and the increase in port isolation in Fig. 7 and Table 3.

It is worth noting that the radiation patterns and peak gains of the proposed MIMO antenna show a slight asymmetry (approx. 2 dB difference in peak gain). Physically, this behavior originates from the asymmetric current path on the ground plane when individual ports are excited sequentially. In a MIMO system, although identical port performance is preferred, this does not severely impair the diversity performance. Due to the orthogonal nature of the deflected patterns, the ECC remains exceptionally low (< 0.0005), which successfully compensates for the gain imbalance and maintains high diversity gain.

The designed MIMO antenna is compared for different per formance metrics with recent related work published in the literature as listed in Table 8. The comparison is based on bandwidth, isolation, gain and antenna size. In line with the results, it is observed that although the 2 patch elements are placed at a distance of 0.25λ, the antenna is close to the designs in the literature given in Table 8 with its minimum isolation values between ports, is better than most of them with its gain value, and better values are obtained than most of the proposed designs with its high bandwidth. The proposed MIMO antenna achieves better isolation with a compact size, and therefore, it could be a suitable applicant for MIMO system applications.

VI. CONCLUSION

In this article, a four-port microstrip MIMO antenna with 1×2 elements in the array structure, low profile, high bandwidth, capable of broadcasting in dual polarization, designed and produced for systems operating at 5G frequencies, was designed and produced, and simulation and production measurement results were compared. In the study, to enable the proposed design to operate in dual polarization, two ports have been positioned orthogonally on the edges of patch antenna. Additionally, for the antenna to have linear polarization and to exhibit equal characteristics in both horizontal and vertical polarizations, the patches were designed in a square shape. To minimize the antenna's footprint, the patch structures were placed at a distance 0.25λ apart, while ensuring that the isolation between the ports remains below -20 dB. The bandwidths of the 4-port antenna were measured as 3.89 GHz, 4.72 GHz, 4.35 GHz, and 3.8 GHz respectively. MIMO antenna parameters of DG > 9.999, ECC < 0.0005, $TARC$ < -10 dB and CCL < 0.1 are achieved in 25 GHz - 26 GHz range. Consistency was observed between the data obtained from measurements and simulation results.

AUTHOR STATEMENT

Plagiarism Check—The article has been scanned with iThenticate and found to be compliant with the journal's plagiarism policy.

Conflict of Interest—There is no conflict of interest with any person/organization.

Ethics Committee Approval—Ethics committee approval is not required for this article.

Use of Artificial Intelligence Tools—In this study, no artificial intelligence tools were used in article writing. All content reflects the original contribution of the author.

Funding—No institutional/financial support was received for this study.

Data availability—The data supporting the findings of this study were generated by the author(s) and may be obtained from the author(s) upon request.

CRediT Author Contribution—In this study, Miraç Er contributed to the development of the research idea, literature review, and writing of the manuscript. Nursel Akçam contributed to the conceptualization of the idea, the assessment of the results, and the proofreading and editing of the manuscript.

REFERENCES

[1] A. Yıldırım, A. İ. Tunalı, "5G nedir?", *Aselsan Dergi*, 111, 2022, 26-30, https://wwwcdn.aselsan.com/api/file/AselsanDergi111Web1_3663.pdf.

[2] O. Onurlu, "5G sistemleri için anten tasarımı", *Yüksek Lisans Tezi*, Hacettepe Üniversitesi Fen Bilimleri Enstitüsü, Ankara, Türkiye, 2021.

[3] W. A. Awan, A. Zaidi, A. Baghdad, "Patch antenna with improved performance using DGS for 28 GHz applications", *International Conference on Wireless Technologies, Embedded and Intelligent Systems (WITS)*, Fez, Morocco, 03-04 April 2019. https://doi.org/10.1109/WITS.2019.8723828.

[4] M. Kösem "5G haberleşme için geniş bant mikroşerit yama anten modellemesi, alttaş seçimi ve gerçeklemesi" *Yüksek Lisans Tezi*, Van Yüzüncü Yıl Üniversitesi Fen Bilimleri Enstitüsü, Van, Türkiye, 2021.

[5] M. Hacımehmet, "X bant mikroşerit halka yama anten tasarımı ve besleme türlerine göre performanslarının değerlendirilmesi", Pamukkale Üniversitesi Mühendislik Bilimleri Dergisi, 28(2), 215-221, 2022. https://doi.org/10.5505/pajes.2021.30632.

[6] S. W. Su., C. T. Lee, F. S. Chang, "Printed MIMO-antenna system using neutralization-line technique for wireless usb-dongle applications", *IEEE Transactions on Antennas and Propagation*, 60(2), 456-463, 2012. https://doi.org/10.1109/TAP.2011.2173450.

[7] R. P. Liu, X. An, H. X. Zheng, M. J. Wang, Z. B. Gao, E. P. Li, "Neutralization line decoupling tri-band multiple-ınput multiple-output antenna design", *IEEE Access*, 8, 27018-27026, 2020. https://doi.org/10.1109/ACCESS.2020.2971038.

[8] D. S. Salgare, S. R. Mahadik, "A review of defected ground structure for microstrip antennas", *International Research Journal of Engineering and Technology*, 2(6), 150-154, 2015, https://www.irjet.net/archives/V2/i6/IRJET-V2I628.pdf.

[9] Rogers Corporation, "RT/duroid® 5870-5880 Data Sheet", https://www.rogerscorp.com/advanced-electronics-solutions/rt-duroid-laminates/rt-duroid-5880-laminates (05.05.2024).

Table 8. References and comparison table of recommended design results.

References	Resonance Frequency (GHz)	Bandwidth (GHz)	Isolation Between Ports (dB)	Gain (dBi)	Antenna Size (mm²)
[10]	3.6	0.2	> 25	8.1	50×25
[19]	3.1 – 11	6.9	> 25	5.67	26×31
[20]	2.6 / 5.4	0.65 / 0.975	> 19.3	3.8	50×50
[13]	2.45 /5.45	0.1 / 0.7	> 15	3	19×23
[26]	13	12.9–13.1	> 25	7.02	35×35
[6]	27.5	3	> 15	7.5	30×65
[21]	29	1	> 20	6	14.4×5.3
[22]	26-31	6	> 21	10	11.3×31
[3]	30.6	1.8	> 25	8.6	60×60
[14]	26	3.56	-	10	-
[17]	28.3	2.15	-	8.1	11×22
[15]	28	0.28	-	2.2	3.494×5.3
[16]	27.91	0.582	-	6.69	11.71×7.9
[23]	28	1.38	-	7.76	16.2×12.8
[24]	30.6	1,8	> 25	8.6	48×21
This study	**25.5**	**4.72**	**> 22.5**	**> 7**	**24×29.58**

[10] A. Ullah, N. O. Parchin, M. Alibakhshikenari, R. A. Abd-Alhameed, A. S. I. Amar, A. I. Salem, "A circularly-polarized patch antenna design for 3.6 GHz applications in 5G systems", *International Telecommunications Conference (ITC-Egypt),* Alexandria, Egypt, 18-20 July 2023, 467-470. https://doi.org/10.1109/ITC-Egypt58155.2023.10206122.

[11] G. Breed, "An introduction to defected ground structures in microstrip circuits", *High Frequency Electronics*, 50-54, 2008, https://api.semanticscholar.org/CorpusID:108194467.

[12] H. Elftouh, N. A. Touhami, M. Aghoutane, S. El Amrani, A. Tazón, M. Boussouis, "Miniaturized microstrip patch antenna with defected ground structure", *Electromagnetics Research C*, 55, 25-33, 2014, https://api.semanticscholar.org/CorpusID:110241105.

[13] M. S. Khan, M. F. Shafique, A. Naqvi, A. D. Capobianco, B. Ijaz, B.D. Braaten, "A miniaturized dual-band MIMO antenna for WLAN applications", *IEEE Antennas Wireless Propagation Letters,* 14, 958–961, 2015. https://doi.org/10.1109/LAWP.2014.2387701.

[14] J. Colaco, R. Lohani, "Design and implementation of microstrip patch antenna for 5G applications", *5th International Conference on Communication and Electronics Systems (ICCES)*, Coimbatore, India, 10-12 June 2020, 682-685. https://doi.org/10.1109/ICCES48766.2020.9137921.

[15] Y. Li, "A microstrip patch antenna for 5G mobile communications", *Journal of Physics: Conference Series*, 2580, 012063, 2023. https://doi.org/10.1088/1742-6596/2580/1/012063.

[16] D. Mungur, S. Duraikannan, "Microstrip patch antenna at 28 GHz for 5G applications", *Journal of Science Technology Engineering and Management-Advanced Research & Innovation*, 1(1), 20-22, 2018.

[17] A. Kumar, S. Das, R. L. Yadava, "DGS and SRR based FSS microstrip antenna for 5G communication", *Proceedings of the 4th International Conference on Computational Intelligence & Communication Technology* (CICT), Ghaziabad, India, 09-10 February 2018. https://doi.org/10.1109/CIACT.2018.8480366.

[18] K. Güvenli, S. Yenikaya, M. Seçmen, B. Emin, "5G uygulamaları için bant-dışı baskılamalı bütünleşik M-YTED filtre-yama anten tasarımı ve üretimi*", Pamukkale Üniversitesi Mühendislik Bilimleri Dergisi*, 30(5), 602-609, 2024. https://doi.org/10.5505/pajes.2023.79438.

[19] A. Khan, S. Bashir, S. Ghafoor, K. K. Qureshi, "Mutual coupling reduction using ground stub and EBG in a compact wideband MIMO-antenna", *IEEE Access*, 9, 40972-40979, 2021. https://doi.org/10.1109/ACCESS.2021.3065441.

[20] Q. C. Yang, C. B. Zhang, Q. B. Cai, T.H. Loh, G. Liu, "A MIMO antenna with high gain and enhanced isolation for WLAN applications", *Applied Sciences*, 12(5), 2279, 2022. https://doi.org/10.3390/app12052279.

[21] A. Ahmad, D. -Y. Choi, S. Ullah, "A compact two elements MIMO antenna for 5G communication". *Scientific Reports*, 12(1), 3608, 2022. https://doi.org/10.1038/s41598-022-07579-5.

[22] Z. Wani, P. M. Abegaonkar, K. S. Koul, "28-GHz antenna for 5G MIMO applications", *Progress in Electromagnetics Research Letters*, 78, 73-79, 2018. https://doi.org/10.2528/PIERL18070303.

[23] K. Cuneray, N. Akcam, T Okan, G. O. Arican, "28/38 GHz dual-band MIMO antenna with wideband and high gain properties for 5G applications. *AEU-International Journal of Electronics and Communications,* 162, 154553, 2023. https://doi.org/10.1016/j.aeue.2023.154553.

[24] M. S. Sharawi, S. K. Podilchak, M. T. Hussain, Y. M. M. Antar, "Dielectric resonator based MIMO antenna system enabling millimetre-wave mobile devices", *IET Microwave Antennas & Propagation*, 11(2), 287–293, 2017. https://doi.org/10.1049/iet-map.2016.0457.

[25] D. Tran-Huy, C. Do-Manh, H. Pham-Duy, N. Tran-Viet-Duc, H. Tran, D. Nguyen-Tien, N. Hussain, "Compact Four-Port MIMO Antenna Using Dual-Polarized Patch and Defected Ground Structure for IoT Devices", *Sensors* 25(14), 4254, 2025. https://doi.org/10.3390/s25144254.

[26] R. Sethumadhavi, B. Mishra, A. K. Singh, D. Yadav, S. Eduru, T.Y. Satheesha, "Dual and wideband mmWave 28/38 GHz quad port MIMO antenna for 5G and beyond applications", *Scientific Reports*, 15(1), 44195, 2025. https://doi.org/10.1038/s41598-025-27924-8.

[27] B. Rezaee, A. Abdi, S. Javadi, W. Bösch "Compact Four- Port Ku Band MIMO Antenna with Enhanced Isolation Using Modified DGS for Early-Phase 6G", *Electronics*, 15(1), 94, 2026. https://doi.org/10.3390/electronics15010094.